Protein Kinase B, P34cdc2 Kinase, and p21 ras GTP-Binding in Kidneys of Aging Rats

VIPUL V. PAREKH,* JEFF C. FALCONE,* LISA A. WILLS-FRANK,† IRVING G. JOSHUA,* JAYDEV N. DHOLAKIA,‡ AND JOHN C. PASSMORE*,[1]

Department of Physiology and Biophysics, †Department of Pathology, and ‡Department of Biochemistry and Molecular Biology, University of Louisville School of Medicine, Louisville, Kentucky 40202

Renal nephropathy present in male Wistar rats more than 13 months of age was reported as an indication that the rats were in renal failure. In this study, the renal tissue damage at 14 months of age in male Munich Wistar rats was similar to that reported for Wistar rats, indicating that Munich Wistar rats could be another model for study of kidney function in the aging rat. The usual renal response to injury involves increased cell division and/or reparative processes that involve tyrosine kinase activity (TyrK) and/or guanosine triphosphate-binding (G) protein signal transduction pathways. This study reveals the presence of renal tissue damage coinciding with significantly reduced activitiy of Ras, Akt, and p34cdc2 kinase, the signaling proteins that regulate cell division and/or growth, in renal cortical tissues of aging rats compared to young rats ($P < 0.005$, $P < 0.005$, and $P < 0.001$, respectively). These results suggest that proteins involved in signal transduction pathways associated with cell replication are downregulated in the aging kidney cortex at a time when renal cellular damage is also present. Exp Biol Med 229:850–856, 2004

Key words: renal pathology; signal transduction; cellular integrity; cell cycling

Introduction

Along with a progressive decline in renal function, humans and rats undergo the development of an observable cytologic renal pathology that occurs with aging. Glomerulosclerosis, interstitial fibrosis, infiltration by inflammatory cells, and tubular casts have been described in the kidneys of aging humans and rats (1–3). Detailed renal pathological changes associated with aging in male Wistar rats have also been described (4). By 13 to 18 months of age, renal disease was described as the cause for 88% of the morbidity found in the studied rats and the cause for 58% of the morbidity found in 19- to 21-month-old rats. The primary histological findings were chronic nephropathy including interstitial fibrosis with lymphocyte infiltrates and tubular dilation and casts (4).

It has been observed that the response of the normal mature adult kidney to injury involves cellular and molecular reparative or replacement processes (5, 6). In a previous study, we found a downregulation of guanosine triphosphate (GTP)-binding (G) protein, $G_{\alpha s}$, tyrosine kinase (TyrK), and mitogen-activated protein kinase (MAPK) in renal cortical tissue of aging rats (7). Downregulation of these important signaling compounds would be expected to result in downregulation of cellular repair and replacement (8). As indicated by the studies in yeast cells, external signals for cell protein production and/or growth include signals from membrane receptors, which suggests that activated TyrK type receptors can activate ras p21 small G protein (Ras) through a son of sevenless intermediate step to propagate signals to activate cytoplasmic kinases including MAPK (9–14). Another pathway can act through G proteins and/or TyrK to activate PI-3 kinase, and the activation of Akt (protein kinase B) is another likely mechanism by which membrane signaling agonists relay activity to the interior of the cell (13, 15–17). Further downstream, cyclins are nuclear regulatory proteins that form complexes with p34cdc2 kinase. Increased activity of p34cdc2 kinase and its association with cyclin B would likely indicate decreased cell replication and/or a decrease in cell regeneration. It is likely that a downregulation in the function of these regulatory signaling agents would result in loss of cell growth and/or turnover. Reduced cellular regeneration would result in a reduction in the proportion of "healthy" cells and therefore the increased occurrence of

This work was supported in part by the National Institute on Aging, American Heart Association–Ohio Valley Affiliate, and University of Louisville Research Initiative Funds.

[1] To whom correspondence should be addressed at Department of Physiology, University of Louisville, 500 South Preston Street, Rm. 1115, Louisville, KY 40202. E-mail: jcpass01@gwise.louisville.edu

Received March 20, 2003.
Accepted April 25, 2004.

1535-3702/04/2298-0850$15.00

cells that appear degraded in the renal cortex of aging male rats.

First, we proposed that if pathocytology occurs as an aging process that is characteristic of rats, then it should be found in more than one strain (Wistar; Ref. 4) and would likely occur in Munich Wistar rats. Second, we proposed that any loss of cellular integrity of structures in the renal cortex that is characteristic of aging in the male Munich Wistar rats would likely occur in spite of upregulation of cellular growth and repair processes. In fact, we hypothesized the presence of a downregulation of those signaling compounds could be associated with reduced cellular repair and replacement.

Materials and Methods

Rationale for Selecting 4-Month-Old Rats as Mature Adult Rats. Beta-1 and beta-2 adrenergic receptors that regulate glucose output are mature in 2- to 3-month-old rats (18), and vascular distribution in the prostate gland is completed in 3-month-old rats (19). Thus, we consider 4 ± 0.5-month-old rats (367 ± 10 g body wt) as young adult subjects that have reached a mature stage of life.

Rationale for Selecting 14-Month-Old Rats as the Aging Group. Previous studies have shown that 14 of 15 male rats develop some chronic renal failure by 12 months of age (4). The primary histological findings in that study were chronic nephropathy, including interstitial fibrosis with lymphocyte infiltrates, and tubular dilation and cysts, which were large and in many cases appearing to lead to hydronephrosis. Therefore, by 14 ± 1 months of age (441 ± 9 g body wt), we expected that renal tissue in male rats would clearly demonstrate areas of loss of renal cellular integrity. In this study, the appearance of renal damage was the primary criteria to distinguish between a young adult and an aging rat.

In the current investigation, Munich Wistar rats were obtained from Simonsen Laboratories (Gilroy, CA) at 3.5 months of age and 8 months of age. Aging of animals was completed in the Animal Care Center at the University of Louisville. Rats were housed individually in an environmentally monitored animal care facility and were provided food and water consumption *ad libitum*. At the time of sacrifice, the rats were administered pentobarbital for anesthesia, 50 mg/kg pentobarbital (i.p.), and placed on a temperature-regulated heating pad during the time of surgery. Every attempt was made to reduce the rat's strain and discomfort prior to and during the surgery. All animal procedures in this study were approved by the Institutional Animal Care and Use Committee at the University of Louisville.

Histology. In anesthetized rats, retrograde cannulation of the abdominal aorta was performed and the circulation of the rat, including the kidney circulation, was flushed with 50 ml of ice-cold phosphate-buffered saline (PBS). The kidneys were removed, weighed, and bivalved along the longitudinal axis. Each half was placed into a tissue cassette. The cassettes were then placed into 10% neutral-buffered formalin for fixation. Further tissue processing included continuation of exposure to fresh 10% neutral-buffered formalin, followed by dehydration of the tissue and clearing of the tissue and finally infiltratration of the tissue with paraffin. The processed tissue was then placed into a paraffin block, sectioned into 5-μm sections, and stained with hematoxylin and eosin as well as periodic acid–Schiff (PAS) stains. Sections were examined for glomerular, tubular, and interstitial changes via observation of hematoxylin and eosin and periodic acid–Schiff stains. Three low-power fields (×4) from each of 4 longitudinal kidney sections were examined for glomerular counts. One field from each pole of the kidney as well as one from midportion of the sample were examined. These counts were averaged to give an average glomerular count per low-power field (lpf) in each kidney. Because all low-power fields would have the same diameter and the thickness of the tissue was the same in all cases, it is reasonable that the average glomerular count/low-power field would be an estimate of the number of glomeruli per standard unit of kidney mass. Twenty random glomeruli from four different areas in the longitudinal section from a given kidney section were measured with an ocular micrometer to determine the average glomerular diameter (in millimeters) per section of tissue. The diameters from each of the four blocks were then averaged to give an average glomerular diameter per kidney.

Renal Cortical Tissue. Rat kidneys flushed with PBS were obtained as described above. Methods of tissue extraction and homogenization were similar to those described previously (7). The kidneys were then decapsulated, and the cortex was separated from the medulla. Cortical tissues were homogenized in a 10 m*M* potassium phosphate buffer at pH 7.7 containing 250 m*M* sucrose, 1 m*M* EDTA, 0.1 m*M* PMSF; 1 mg/ml each of leupeptin, pepstatin A, and aprotonin; and 0.25% Triton-X 100. The homogenates were centrifuged at 3,000 *g* at 4°C to remove large particles and then at 15,000 *g* for 45 mins to separate membranes from cytosolic fractions. Supernatants were kept frozen at −70°C until ready to be analyzed. Protein was measured by using Bio-Rad protein assay reagent (Bio Rad, Hercules, CA) using bovine serum albumin as a standard.

Immunoblotting To Determine Ras. The procedure for Western blotting was similar to that previously published with some modification (7, 20). Approximately 200 μg of supernatant protein from the homogenates of renal cortex were incubated in sodium dodecyl sulfate (SDS) sample buffer at 95°C for 5 mins. Proteins were separated by 12% sodium dodecyl sulfate-polyacrylamide gel electrophoresis (SDS-PAGE.) Protein standards of known molecular weight markers (Bio-Rad) and a positive control of the appropriate protein were concurrently run. Proteins were then transferred to polyvinylidene difluoride (PVDF) membranes using a Mini-Transblot (Bio-Rad).

Blots were incubated in a blocking solution (6% nonfat dry milk) at room temperature. Following two washes with TTBS (15 m*M* Tris-HCl; pH 8.0, 160 m*M* NaCl, and 0.05% Tween-20), PVDF membranes were incubated overnight at 4°C with a rabbit polyclonal IgG antibody specific for Ras (Santa Cruz, Santa Cruz, CA). The PVDF membranes were then incubated with anti-rabbit antibody, followed by two subsequent washes in TTBS. Proteins were then developed with enhanced chemiluminescence (Amersham, Piscataway, NJ) and analyzed by a densitometer (STORM, Molecular Dynamics, Sunnyvale, CA) to detect and quantitate the enhanced chemiluminescence.

Protein GTP/(GTP + GDP) Binding Assay for Ras. The assay was performed by a technique that was previously published with some modifications (7, 21). Approximately 200 μg of protein from renal cortical homogenates were incubated at 4°C for 10 mins in a reaction buffer containing 20 m*M* Tris HCl, pH 7.5, 10 m*M* $MgCl_2$, 400 m*M* NaCl, 2 m*M* DTT, and 2 m*M* L-α-phosphatidylcholine dimyristoyl (DMPC). [α-^{32}P]GTP (0.1 mCi/l) was added to the reaction mixture and incubated at 37°C for 30 mins. The samples were then immunoprecipitated with Ras antibody conjugated to agarose beads at 4°C for 1 hr and then centrifuged at 14,000 *g*. Pellets were washed and resuspended in 50 μl of elution buffer (2 m*M* EDTA, and 1 m*M* DTT) to which 0.5 m*M* each of guanosine diphosphate and GTP and 0.1% of SDS was added. The samples were incubated at 80°C for 5 mins, and 30 μl of each supernatant was spotted on thin layer chromatography (TLC) plates (EMD Chemicals, Gibbstown, NJ) and developed with a mobile phase (1.2 *M* ammonium formate and 0.8 *M* HCl). Plates were dried, and a phosphorimager was used for quantitative analysis (STORM, Molecular Dynamics).

Protein Kinase B Assay (Akt). Protein kinase B was immunoprecipitated, and the immunoprecipitate was assayed for the rate of phosphorylation of myelin basic protein (MBP). Supernatants of the kidney cortical tissue homogenates containing approximately 200 μg of protein were incubated for 2 hrs at 4°C with 2 μg of agarose conjugated affinity-purified polyclonal antiserum. Samples were then incubated for an additional 2 hrs at 4°C. After a brief centrifugation at 10,000 rpm for 60 secs, pellets were washed 3 times with 1 ml of immunoprecipitation buffer (50 m*M* Tris HCl, 250 m*M* NaCl, 5 m*M* sodium pyrophosphate, 1 m*M* sodium orthovanadate, and 1 m*M* PMSF, pH 7.4). The final wash of the pellet was done in kinase buffer (50 m*M* Tris, 10 m*M* $MgCl_2$, 1 m*M* DTT, and 0.4% betamercaptoethanol pH 8). To assay Akt, the resuspended immunoprecipitates were incubated at 33°C for 8 mins in a final volume of 50 μl of kinase buffer containing 6 μg of myelin basic protein and 6 μCi of [γ32-P]ATP (specific activity 3000 Ci/mmol, [New England Nuclear, Boston, MA]). The reaction was terminated by addition of SDS sample buffer. The samples were then electrophoresed on a 12% SDS-PAGE gel. Gels were dried and exposed to Kodak film. To obtain relative numerical values in this assay, radioactivity was also quantitated using a densitometer employing a phosphoimager screen (Molecular Dynamics, Chicago, IL).

P34cdc2 Kinase Assay. Activity was measured by a method that was previously published (22–24). In brief, p34cdc2 kinase was immunoprecipitated, and the immunoprecipitate was assayed for the rate of phosphorylation of histone H1. Immunoprecipitations were carried out using antiserum against a synthetic peptide corresponding to the carboxyl terminus of the human cdc2 protein. Supernatants of the kidney cortex homogenates containing approximately 200 μg of protein were incubated for 2 hrs at 4°C with 2 μg of affinity-purified polyclonal antiserum. This was followed by addition of 4 mg of hydrated protein-A-sepharose (Sigma, St. Louis, MO). Samples were then incubated for an additional 2 hrs at 4°C. After a brief centrifugation at 10,000 rpm for 60 secs, pellets were washed 4 times with 1 ml of immunoprecipitation buffer (50 m*M* Tris HCl, 250 m*M* NaCl, 5 m*M* sodium pyrophosphate, 1 m*M* sodium orthovanadate, and 1 m*M* PMSF, pH 7.4). The final wash of the pellet was done in kinase buffer (50 m*M* Tris, 10 m*M* $MgCl_2$, and 1 m*M* DTT, pH 8). To assay p34cdc2 kinase the resuspended immunoprecipitates were incubated at 33°C for 8 mins in a final volume of 50 μl of kinase buffer containing 6 μg histone H1 and 6 μCi of [γ-32P]ATP (specific activity 3000 Ci/mmol, New England Nuclear). The reaction was terminated by the addition of SDS sample buffer. The samples were then electrophoresed on a 12% SDS-PAGE gel. The commercial preparation of histone H1 used as a substrate gave 2 phosphorylated products at approximately 34 kDa, and untreated histone H1 electrophoresed and stained with Coomassie blue showed the same 2 bands (data not shown). Gels were dried and exposed to Kodak film. To obtain relative numerical values in this assay, radioactivity was also quantitated using a densitometer employing a phosphoimager screen (Molecular Dynamics).

Amount of p34cdc2 Kinase Associated with Cyclin B. In this case, 2 μg of an antibody against cyclin B was used to immunoprecipitate this protein and any bound p34cdc2 kinase. Immunoprecipitation and assays were carried out as above.

Statistical Analysis. Values in graphs and tables shown are mean ± SEM. Significance was determined using analysis of variance (ANOVA) test. The unpaired Student *t* test was used to determine statistical significance between corresponding mean values. Values of $P < 0.05$ were considered to indicate statistically significant differences between the corresponding mean values.

Results

Figure 1 (top left) demonstrates an area of damage in the kidney cortex of a 15-month-old male Munich Wistar rat. Compared to the tissue from the 4-month-old rat (top right of Fig. 1), the glomerulus in the older rat demonstrates

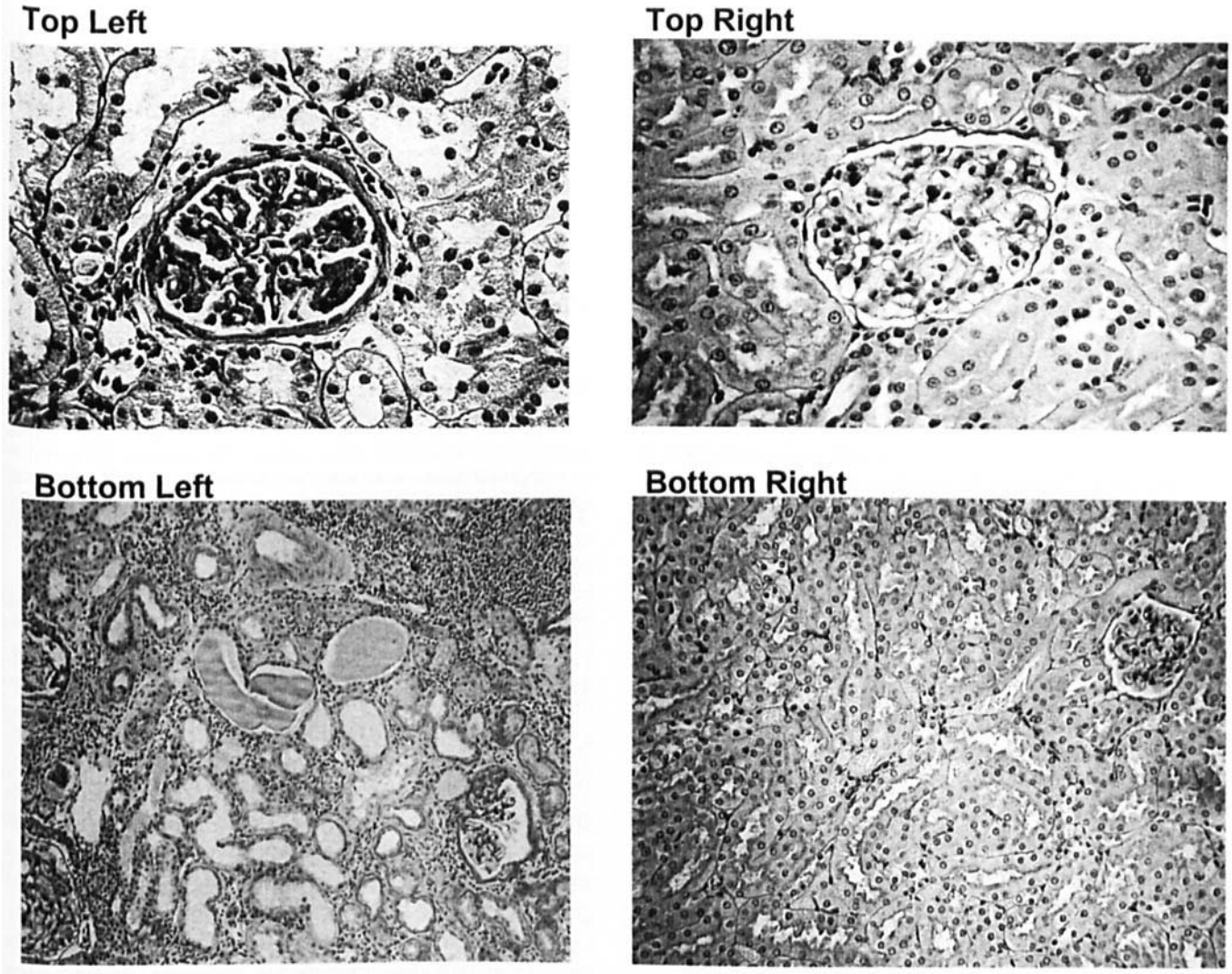

Figure 1. (Top left) A photomicrograph of renal cortical tissue from a 15-month-old male rat demonstrating an example of focal glomerular wrinkling, the dark periodic acid–Schiff staining, and thickening of the glomerular membrane.suggesting that glomerular sclerosis has started. The capillaries are also distorted. The top-right photomicrograph is from a 4-month-old rat to illustrate a "normal" condition. The bottom-left photomicrograph is of renal cortical tissue taken from a 15-month-old male rat. This picture demonstrates the dilated tubules filled with plaque-like material and the leukocyte infiltration that are characteristically found in male Munich Wistar rats of this age. The bottom-right photomicrograph is from a 4-month-old rat to illustrate a "normal" condition.

damaged capillaries with dark PAS staining. The staining indicates that some sclerosis is present. The capsule is also thickened. The surrounding tubules appear to have less brush border than those of the younger rat. Figure 1 (bottom left) demonstrates an area of tubular damage in the cortex of a 15-month-old male Wistar rat. There are enlarged tubules filled with a plaque-like material and areas of leukocyte infiltration not seen in the tissue from the 4-month-old rat (bottom right of Fig. 1).

As seen in Table 1, body weight of the rats increased in a manner appropriate to the Munich Wistar rat strain, demonstrating an increase of approximately 20% between 4 months and 14 months of age, whereas kidney weight increased approximately 38% between 4 months and 14 months of age. The number of glomeruli per lpf decreased

Table 1. Body Weights and Kidney Values[a]

Age of male MW rats	Body weight (g)	Kidney weight (g)	Glomeruli/lpf	Glomerular diameters (mm)
4 months old	367 ± 10	1.04 ± 0.03	57 ± 5	0.11 ± 0.05
14 months old	441 ± 9	1.43 ± 0.06	39 ± 4	0.15 ± 1

[a] Fourteen-month-old rats were larger, had increased kidney weight, had fewer glomeruli/lpf, and had larger glomerular diameters than those of the 4-month-old rats ($P < 0.01$, $P < 0.01$, $P < 0.05$, $P < 0.05$, respectively). MW, Munich Wistar; lpf, low-power field.

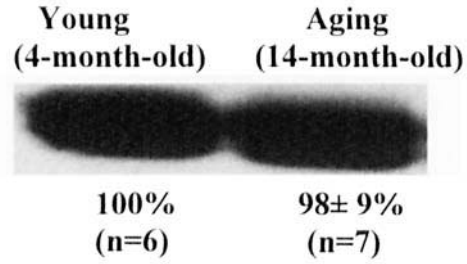

Figure 2. The quantification (Western blot) of H-ras in the homogenates of kidney cortex of young and aging rats. Value for the aging rat is represented as a percentage of the mean of the young rat value (100%). Value for the older rats is presented as the mean ± SEM of calculated values. Homogenates from kidney cortex of 14-month-old rats had similar quantities of H-ras when compared to the homogenates of kidney cortex or 4-month-old rats.

approximately 32% between 4 months and 14 months of age. However, because the kidneys increased in weight, the total number of glomeruli per kidney did not appear to change. Glomerular diameters were increased in the older rats ($P < 0.05$).

Homogenates from the kidney cortex of 14-month-old rats had similar quantities of H-ras when compared to the homogenates of kidney cortex of 4-month-old rats (Fig. 2). The steady-state ratio of bound GTP for Ras was significantly decreased in the renal cortical tissue of the aging rats compared to young rats ($P < 0.005$; Fig. 3).

The relative levels for Akt activity in the homogenates from kidney cortex of 4-month-old and 14-month-old rats are demonstrated in Figure 4. Homogenates from kidney cortex of 14-month-old rats showed significantly lower Akt activity compared to 4-month-old rats ($P < 0.005$).

The relative numerical values for the results of the gel electrophoretic analysis of histone H1 phosphorylation by p34cdc2 kinase are summarized in Figure 5. In the young rat, there is a relative association between p34cdc2 kinase and cyclin B. There was a significant decrease in the activity of p34cdc2 kinase in the kidney cortex of aging rats compared to the kidney cortex of young adult rats ($P <$ 0.001) and, in addition, a similar decrease of cyclin B was found ($P < 0.001$ vs. younger rats; Fig. 5)

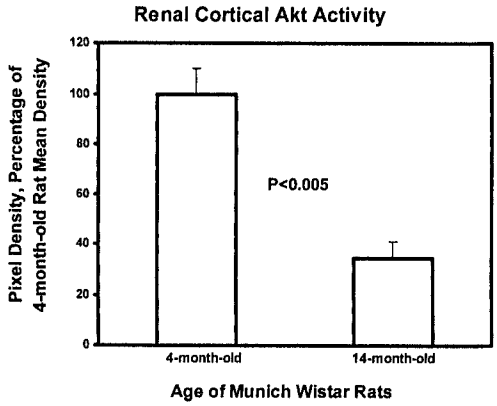

Figure 4. Akt activity (phosphorylation of myelin basic protein by Akt) in the homogenates from kidney cortex of 4-month-old ($n = 6$) and 14-month-old ($n = 7$) rats is represented. The average value for the younger rats represents 100% activity. The average value of the younger rats was used as the reference for calculating the percentage values for aging rats. Older rats had significantly decreased activity compared to 4-month-old rats ($P < 0.05$). Values shown are mean ± SEM.

Discussion

This study demonstrates that renal cortical tissue damage during aging in Munich Wistar rats is similar to that reported in Wistar rats (4). In these Munich Wistar rats, the damage in focal areas was found to be extensive with enlarged and sclerotic glomeruli and wrinkled, damaged capillary tufts. Tubules were dilated and filled with a plaque-like material. Leukocyte infiltration was present.

Signals for repair or replacement of damaged cells include signals from membrane receptors. It has been indicated, from studies in yeast cells, that activated TyrK type receptors can activate ras p21 small G protein (Ras) through a son of sevenless intermediate step to propagate signals to activate cytoplasmic kinases including MAPK (9–

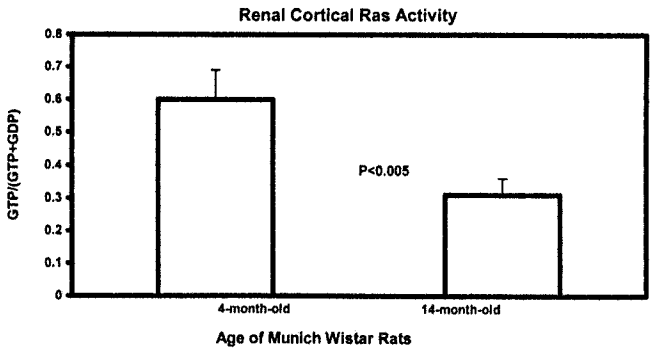

Figure 3. GTP/GDP binding activity of H-Ras in homogenates from the kidney cortex of young ($n = 6$) and aging ($n = 7$) rats. The average value for the younger rats was used as the reference for calculating the percentage values for aging rats. Older rats had significantly decreased activity compared to 4-month-old rats ($P < 0.05$). Values shown are mean ± SEM.

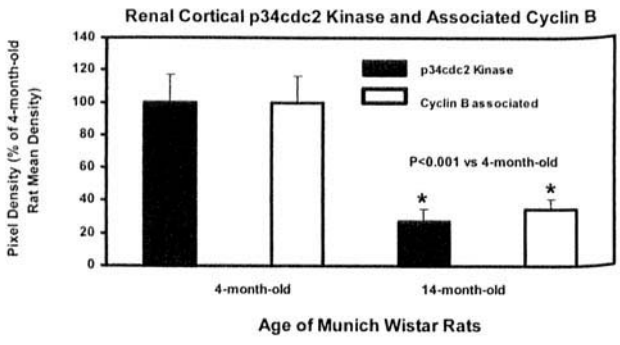

Figure 5. Represents P34cdc2 kinase activity in the homogenates of kidney cortex of young and aging rats. Values of young ($n = 6$) represent 100% activity. The average value for the younger rats was used as the reference for representing the percentage values for aging rats. Values shown are mean ± SEM. Older rats had significantly decreased activity compared to 4-month-old rats ($P <$ 0.001 for both).

14). Another pathway can act through G proteins and/or TyrK to to activate PI-3 kinase. Activation of Akt is also a likely mechanism by which membrane signaling agonists relay activity to the interior of the cell (13, 16, 17).

Cyclins are nuclear regulatory proteins that form complexes with p34cdc2 kinase. Increased activity of p34cdc2 kinase and its association with cyclin B signals cell replication, whereas downregulation of this pathway could lead to decrease in cell regeneration. Previously, we reported that the activities of TyrK, $G_{\alpha s}$, MAPK, and autophosphorylation of MAPK were decreased, whereas the activity of $G_{\alpha}i$ was increased in the aging kidney cortex (7). In the current study, we further demonstrate that the activity of Ras, p34cdc2 kinase (total and cyclin B–associated), and Akt were decreased in the kidneys of aging rats compared to young rats, suggesting that the signal transduction pathways associated with renal cell regeneration are downregulated and may be associated with a reduction in the activity of the downstream effectors that cause cell regeneration.

These results were consistent with our previous findings in the jejunum of the small intestine, where we found that the activities of cytoplasmic and nuclear kinases associated with cell regeneration declined significantly with mucosal cell exfoliation and hypoplasia. (22–24). Other studies have shown that exposure of MCF-7 breast cancer cells to insulin-like growth factor (IGF) induces proliferation as a result of activation of the PI-3 kinase–Akt pathway and, subsequently, activation of Ras-Raf-MAPK pathways (25). They also found that prolonged activation of the Ras-MAPK pathway cascade inhibits growth in these cells. Thus, regulation of the Ras-MAPK pathway in MCF-7 breast cells determines whether the response is proliferation or growth arrest. Those results are consistent with our current investigation, where we found that downregulation of Akt activity is associated with decrease in the Ras–GTP-binding pathway and could result in decreased cell growth and/or replacement. With downregulation of Ras, TyrK, Akt, and p34cdc2K activity, a likely scenario would be that cells remaining after the loss of cellular components of nephrons in aging kidneys may be less able to regenerate.

Combining our previous and current studies, we summarize that there are no significant changes in the quantity of $G_{\alpha}s$ and Ras even though there was a significant decline in their activity and a decline in TyrK activity in aging kidneys. These results suggest a downregulation of the capacity of these proteins to translate extracellular signals, which would result in a decrease in the activity of the signal transduction pathways important for cellular regeneration.

We have chosen to examine the activities of Akt, p34cdc2 kinase and the amount of p34cdc2 associated with cyclin B and found evidence of downregulation further downstream. There are many other pathways that could be investigated and many more functions of these molecules that can be studied; however, the data reported here suggests a downregulation of these important kinases at a time when areas of tissue damage are occurring in the kidney. It is notable that these kinases would be upregulated if kidney damage were to occur in younger animals by insults not related to aging.

The histological studies reported here demonstrate the presence of focal tubular dilation and thus evidence of tubular dysfunction in Munich Wistar rats. An occasional glomerulus demonstrated thickening or wrinkling of the glomerular membranes. Male Wistar rats at this age have been reported to be susceptible to developing renal disease (4). As shown in the photomicrographs, there are focal points of what appears to be damaged glomeruli, glomerular capillaries, tubules, and areas of leukocyte infiltration. Literally all cells in these areas appear to be damaged with aging, making it difficult to correlate between our biochemical results and any specific tissue.

Thus, we conclude based on histology that the Munich Wistar rat can be used as a model to for aging studies in the rat kidney as has been shown for Wistar rats. We also conclude that there is a downregulation in the cytoplasmic and nuclear signaling mechanisms known to be responsible for cellular regeneration in the aging kidney cortex. A decline in cellular regeneration would likely be involved in the decline of renal cell integrity and function that occurs with aging in rats.

1. Lindeman RD. Renal physiology and pathophysiology of aging. In: Sessa A, Battine G (Eds). Glomerulonephritis in the Elderly. Contrib Nephrol 105:1–12, 1993.
2. Takeda T, Imada A, Horiuchi A, Kimura M, Maekura S, Hashimoto S. Age-related changes in morphological studies in rat and human kidney (Japanese). Nippon Jinzo Gakki Shi (Japanese J Nephrol) 38:555–562, 1996.
3. Thomas SE, Anderson S, Gordon KL, Oyama TT, Shankland SJ, Johnson RJ. Tubulointerstitial disease in aging: evidence for underlying peritubular capillary damage, a potential role for renal ischemia. J Am Soc Nephrol 9:231–242, 1998.
4. Roth GS, Brennecke LH, French AW, Williams NG, Waggie KS, Spurgeon HA, Ingram DK. Pathological characterization of male Wistar rats from the gerontology research center. J Gerontol: Biol Sci 48:B213–B230, 1993.
5. Safirstein R, DiMari J, Megyesi J, Price P. Mechanisms of renal repair and survival following acute injury. Semin Nephrol 18:519–522, 1998.
6. Spiegel AM, Weistein LS, Shenker A. Abnormalities in G-protein coupled signal transduction pathways in human disease. J Clin Invest 92 1119–1125, 1993.
7. Parekh VV, Maier KG, Roman RJ, Joshua IG, Falcone JC, Passmore,JC. Altered expression and activity of G-proteins, mitogen activated protein kinases (MAP-K) and tyrosine kinases in aging kidney cortex. J Invest Med 47:462–467, 1999.
8. Schuchardt A, D'Agati V, Larsson-Blomberg L, Costantini F, Pachnis V. RET-deficient mice: an animal model for Hirschsprung's disease and renal agenesis. J Intern Med 238:327–332, 1995.
9. Cantley LC, Auger KR, Carpenter C, Duckworth B, Graziani A, Kapeller R, Soltoff S. Oncogenes and signal transduction. Cell 64:281–302, 1991.
10. Feig LA. The many roads that lead to Ras. Science 260:767–768, 1993.
11. Saifeddine M, Laniyonu A, Ahmad S, Hollenberg MD. Bi-directional

control of smooth muscle tension: regulation by tyrosine kinase and tyrosine phosphatase. Proc Western Pharmacol Soc 37:21–24, 1994.
12. Davis RJ. The mitogen-activated protein kinase signal transduction pathway. J Biol Chem 268:14553–14556, 1993.
13. Abram CL, Courtneidge SA. Src family tyrosine kinases and growth factor signaling. Exp Cell Res 254:1–13, 2000.
14. Howe LR, Leevers SJ, Gomez N, Nakielny S, Cohen P, Marshall CJ, Activation of the MAP-K pathway by the protein kinase raf. Cell 71:335–3342, 1992.
15. Margolis B, Skonik EY. Activation of ras by receptor tyrosine kinases. J Am Soc Nephrol 5:1288–1299, 1994.
16. Hemmings BA. Akt signaling: linking membrane events to life and death decisions. Science 275:628–630, 1997.
17. Krasilnikov MA. Phosphatidylinositol-3 kinase dependent pathways: the role in control of cell growth, survival, and malignant transformation. Biochemistry 65(1):59–67, 2000.
18. Van Ermen A, Van de Velde E, Vanscheeuwijck P, Fraeyman N. Influence of age on the β_1 and β_2 adrenergic receptors in rat liver. Mol Pharmacol 42:649–655, 1992.
19. Skolnik M, Tykochinsky G, Servadio C, Abramovici A. The development of vascular supply of normal rat prostate during the sexual maturation: an angiographic study. Prostate 21:1–14, 1992.
20. Shanahan C, Deasy M, Ravid R, O'Neill C. Comparative immunoblot analysis of the guanine nucleotide binding protein Gq alpha in control and Alzheimer's disease brains. Biochem Soc Trans 23:363S, 1995.
21. Satoh T, Endo M, Nakafuku M, Nakamura S, Kaziro Y. Platelet derived growth factor stimulates formation of active $p21^{ras}$ GTP complex in Swiss mouse 3T3 cells. Proc Natl Acad Sci U S A 87:5993–5997, 1990.
22. Parekh VV, Hoffman JL, Younoszai MK. Effects of diabetes and difluoromethyl ornithine treatment on hyperplasia, activity of MAP-kinase, and activity and association with cyclin B of p34cdc2 kinase in rat jejunal mucosa. J Invest Med 46:76–81, 1998.
23. Parekh VV, Hoffman JL, Younoszai MK. Role of tyrosine kinase, odc, and p34cdc2 kinase and cyclin B associated cdc2 in jejunal enterocyte proliferation, maturation and exfoliation in diabetic and DFMO treated rats. J Invest Med 47:1–9, 1999.
24. Lock R, Keeling P. Responses of HeLa and Chinese Hamster Ovary p34cdc2/cyclin-B kinase in relation to cell cycle perturbations induced by etoposide. Int J Oncol 3:33–42,1993.
25. Albas J, Slager-Davidov R, Steenbergh PH, Sussenbach JS, Vander Burg B. The role of MAP kinase in TPA-mediated cell cycle arrest of human breast cancer cells. Oncogene 16:131–139, 1998.